Intensive plastic deformation of pre-sintered Al powder

Lenka KUNČICKÁ[a], Martin POHLUDKA[a], Terry C. LOWE[b], Casey F. DAVIS[b], Jan JUŘICA[a], Libor HLAVÁČ[a]

a Regional Materials Science and Technology Centre, VŠB-TU Ostrava, 17. listopadu 15, Ostrava-Poruba, 70833, Czech Republic

b The George S. Ansell Department of Metallurgical & Materials Engineering, Colorado School of Mines, Golden, Colorado, 80401 USA

Abstract

The influence of intensive plastic deformation on compacted Al powders was evaluated. The samples subjected to deformation processing were prepared from powder particles with diameters between 25 and 45 μm, pre-compacted using double-step cold isostatic pressing (CIP) at 200+300 MPa applied for 30 seconds each and subsequently vacuum sintered at 500°C for 60 min. Analyses of chemical composition of the sintered samples were carried out using scanning electron microscopy, while microhardness measurements were performed to evaluate the degree of compaction. The results showed increasing microhardness with increasing total imposed strain. Greater refinement of microstructure was achieved by increasing degrees of processing.

Keywords: intensive plastic deformation, swaging, HPT, aluminum powder, hardening

1. INTRODUCTION

Methods of intensive plastic deformation have recently spawned broad interest especially due to their favourable influence on mechanical properties of materials. These methods include for example swaging [1], multiaxial forging [2], and severe plastic deformation (SPD) technologies, such as high pressure torsion (HPT) [3], equal channel angular pressing (ECAP) [4], ECAP-Conform [5], twist channel angular pressing (TCAP) [6], twist channel multi-angular pressing (TCMAP) [7], twist extrusion (TE) [8], repetitive corrugation and straightening (RCS) [9], friction stir processing (FSP) [10], accumulative roll bonding (ARB) [11] and many more.

The increase in mechanical properties, namely strengthening, is caused by a high amount of shear strain imposed into the material during the deformation processing [12]. Shear strain is especially important for consolidation of particles. It is very effective during arrangement of the particles within the volume of the sample, since by its influence smaller particles can effectively fill free volumes between larger particles. Moreover, it supports shearing of the particles and therefore refinement of structural units, which subsequently leads into a more refined structure of the final deformed material. Although strain imposed into the material during one pass (or revolution) is limited, all of the above mentioned processes can be performed repetitively. Therefore the strain can be accumulated during multiple passes. However, this is applicable only to a certain point, in which the material reaches a saturated steady state and the properties do not increase any more with increasing strain [13].

This study is focused on investigation of the influence of methods of intensive plastic deformation, swaging and HPT, on microstructure of material consolidated from Al powder. Analyses consisted of microstructural observations performed using scanning electron microscopy (SEM) and measurements of microhardness. Analyses were supplemented with calculation of degree of deformation for both the methods. Mechanical properties of the sintered material before deformation were measured by the IMCE n.v. company in Belgium.

2. EXPERIMENT

The selected particle size was in the range of 25-45 μm. These particles were compacted using cold isostatic pressing (CIP), first pressurizing at 200 MPa for 30 seconds dwell and then gradually depressurizing. All the samples were compressed in our own fabricated rubber die using a CIP device located at Technical University of Ostrava (TUO). The compacted samples had a diameter of approximately 22 mm. Although the initial dies for both the intensive plastic deformation technologies have the diameter of 20 mm, we designed the rubber mould for powder particles with a larger diameter, since we expected shrinkage of the powder during compaction and subsequent sintering. The samples were sintered at 500°C for 60 minutes in a Zwick vacuum creep testing furnace at ASCR, Brno.

After having performed the compression and sintering steps, the specimens were subjected to intensive plastic deformation at TUO. One 6 mm thick specimen was deformed by one revolution of HPT at room temperature, 5 GPa pressure and 0.5 RPM, while another 6 mm thick specimen was subjected to swaging in 4 subsequent steps, from the initial diameter of 20 mm to a final diameter of 10 mm. The individual swaging steps were performed at room temperature without any heat treatment. After the deformation procedures, the specimens were analysed and compared to the state before deformation.

Energy Dispersive Spectroscopy (EDS) and Back-Scattered Electron (BSE) SEM analyses were performed at TUO to observe the chemical composition of the initial powder and to observe pores in the structure of the deformed samples, while electron backscattered diffraction (EBSD) observations were carried out at the Colorado School of Mines (CSM), Colorado, USA. Samples for the analyses were ground and polished mechanically and eventually ion milled with a JEOL CP Cross Section Polisher. The observed locations for both the samples were in the middle of radius on the cross-section. Microhardness measurements were performed using a Vickers microhardness measuring device at TUO. The samples were subject to a load of 250 g for 7 seconds. Average microhardness was calculated from multiple measurements at 1 mm spacings along a diameter for the swaged sample and the HPT sample in order to investigate possible inhomogeneities throughout the cross-section. Mechanical properties of the sintered material, such as Young's and shear moduli etc., were measured by the IMCE n.v. company in Belgium using a RFDA measuring system (http://www.imce.eu/) in accordance with the ASTM E 1876 standard. All the measurements were performed ten times, from which average values were then calculated.

3. RESULTS AND DISCUSSION

3.1. Chemical composition and mechanical properties of sintered material

According to the EDS analysis, the sintered aluminum samples contained 4.97 wt.% of oxygen. Before swaging and HPT processing, the sintered material was subjected to analyses of several mechanical properties. The results of the measurements are summarized in Table 1. As is evident from the table, the elastic and shear moduli are lower than theoretical moduli for pure aluminum. This is most probably caused by residual porosity in the samples, since porosity decreases moduli of materials [14]. In our experiment, the elastic modulus of the sintered sample is approximately 77% of the theoretical value for Al (70 GPa). The measured Poisson ratio indicate homogenous isotropic behaviour during loading [15]. The table further summarizes several other intrinsic material properties, such as torsion and flexural parameters.

Table 1 Results of measurements of mechanical properties for sintered Al.

Property	*Elasticity modulus [GPa]*	*Shear modulus [GPa]*	*Poisson ratio [-]*	*Flexural Frequency [Hz]*	*Damping Flex. [-]*	*Torsion Frequency [Hz]*	*Damping Torsion [-]*
sintered Al powder	53.98	19.94	0.353	8313.78	0.003035	4725.34	0.000523

3.2. Microstructure

Observations of microstructure were performed in order to investigate differences after processing with the two deformation methods. As regards the influence of the performed deformation technologies on the degree of consolidation and remaining porosity in the samples, this is documented in Figs. 1a and 1b. HPT processing is considered to be the most effective from the point of view of consolidation of powder particles due to the influence of severe shear strain. The reason for this is a favourable positioning of the axis of compression, which is parallel to the axis of shear [12]. This design of the process enables a high intensity of shear strain to be introduced into the material. Mutual comparison of the figures proves better consolidation after HPT, than after swaging.

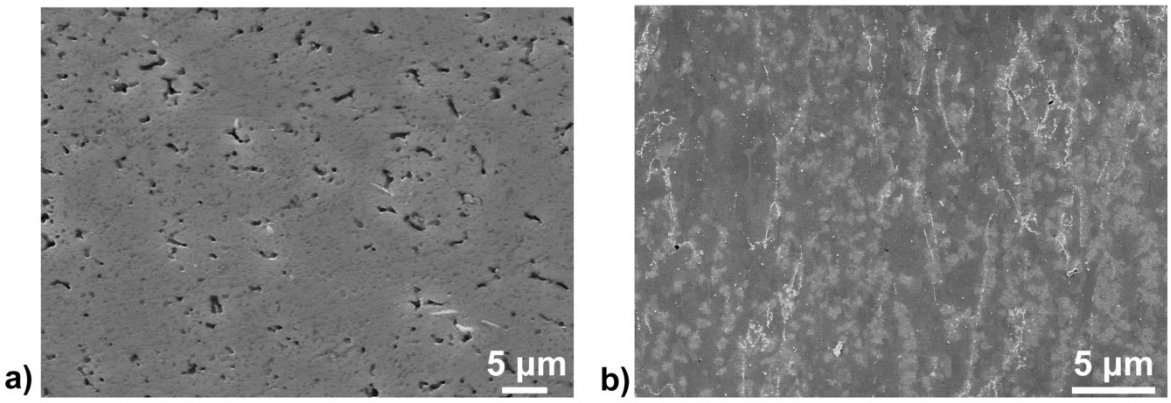

Fig. 1 Microstructures of swaged sample (a), sample after HPT (b).

Grain sizes and orientations after swaging are depicted in Fig. 2a, while microstructure after HPT can be seen in. Fig 2b. As can be seen in the figures, the grains were more significantly refined in the sample deformed by HPT. The grains after swaging and HPT also exhibit different shapes. In the structure of the swaged sample the grains are more elongated, which is caused by the nature of the swaging process during which flow of material along its axis is the only unconstrained direction [16]. The pressure conditions during HPT are close to hydrostatic, therefore the grains tend to maintain a more or less equiaxed shape [17]. Moreover, the orientations of grains are different and more random than in the swaged sample. Most of the grains in the swaged sample are oriented in the <111> fibre direction, while in the sample after HPT only a minor fraction of grains is oriented in this direction. Most of the grains are more randomly oriented, including other directions, i.e. <101> and <001>.

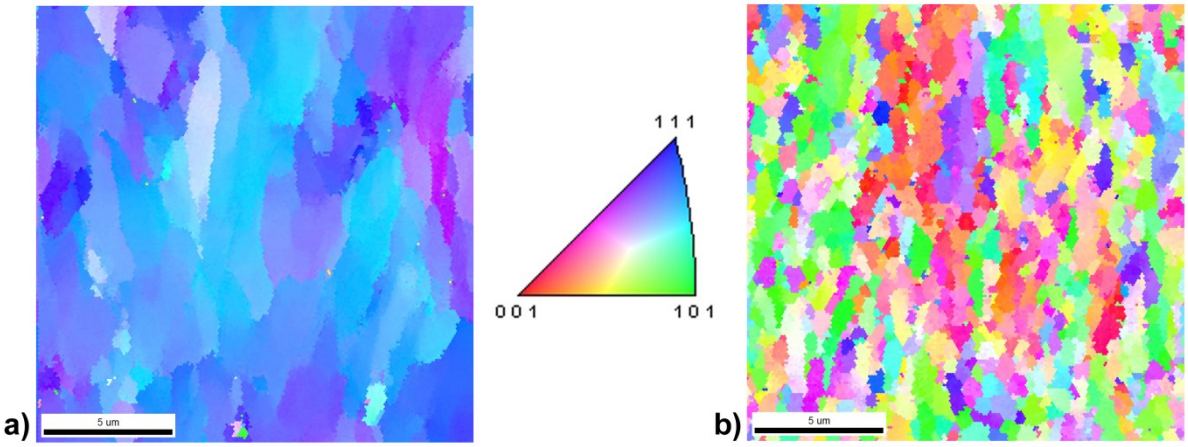

Fig. 2 OIM images of swaged sample (a), sample after HPT (b).

3.2. Microhardness

At first, the average microhardness for the pre-compressed samples after double-step CIP processing was measured. The average value, calculated from values obtained using a line analysis with the spacing of 1 mm throughout the cross-section of the samples, was determined to be 42.86 HV. The measurements did not exhibit any increasing/decreasing trend towards the axis of the pre-compacted samples. Therefore the compression after CIP can be considered to be homogenous throughout the un-deformed material.

Microhardness after HPT was measured along a line passing through the cross-section of the deformed sample. Measurement was performed at 20 individual points starting at the distance of 0.5 mm from the edge of the sample with a spacing of 1 mm. The analyses were performed along top, bottom and central horizontal lines. Results of the measurements are summarized in Figure 3.

The results exhibit trends typical for HPT processing [18]. Throughout the horizontal direction, the lowest values of microhardness can be observed in the central area in the vicinity of the rotational axis of the sample. This is due to the character of HPT processing, during which a die rotates along the central axis and therefore imposes the smallest shear deformation into the central parts of the deformed sample. Considering the vertical direction towards the surfaces of the sample being in contact with the dies, the deformation in the areas closest to the surface of the dies is the highest since the shear is supported by the influence of friction. The imposed strain then slightly decreases towards the internal volume of the sample along the vertical direction, while it increases again along the central horizontal layer.

Notable is also the occurrence of several deviations from the above described trends. However the amount of shear strain introduced into the material is a significant factor influencing hardness of the deformed material, the differences between the amounts of shear strain throughout the cross-section of the sample are not the most important [19]. More significant factor influencing local hardness is the structural nature of the individual measured location. Therefore, the local deviations are most probably caused by pores remaining in the structure. Comparing the top and bottom lines influenced by the surface contact of the specimen with the dies, the average microhardness value for the bottom line in slightly higher than for the top line. This is most probably caused by the HPT process, during which only the bottom die rotates and therefore shear strain could be expected to be more intense in the vicinity of this die.

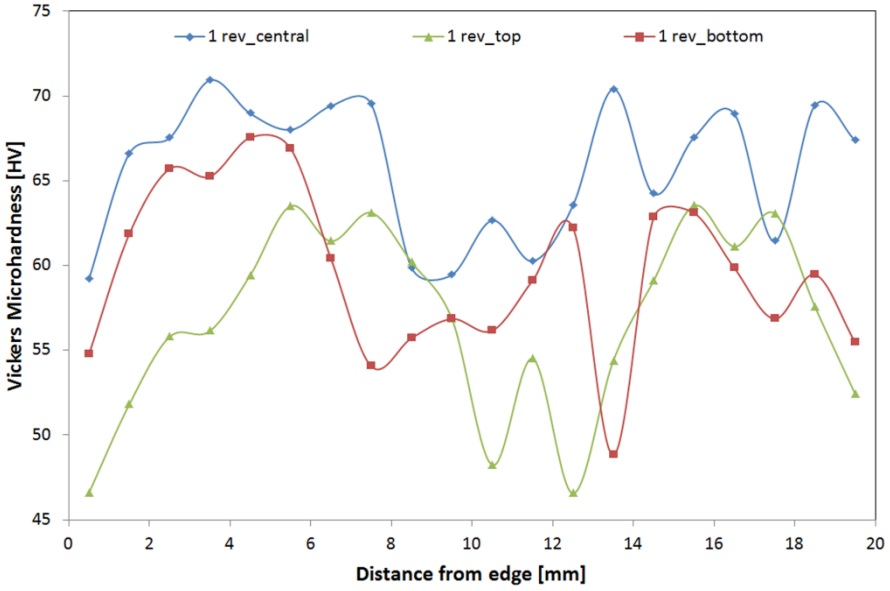

Fig. 3 Microhardness values for HPT processed specimens.

Microhardness was also measured for the specimen after swaging. Although the microhardness for this specimen was also measured along its diameter, the values were more or less uniform and did not exhibit any increasing/decreasing trend towards the centre of the sample. Therefore only the average value was calculated. This was 50.14 HV. When compared to the HPT processed sample, the value is lower than the average values measured for the sample after HPT. This is connected with the amount of imposed deformation, which is substantially higher in the sample deformed by HPT.

Calculations of degree of deformation were performed for swaging (Eq. (1)), as well as for HPT (Eq. (2)) [1,20,21]. According to these calculations, the average strain imposed into the material during swaging was 1.386, while during HPT it was 5.24 for the observed mid-radius location.

$$\varphi = ln\frac{S_0}{S_n} \tag{1}$$

$$\varphi = \frac{2\pi rN}{t} \tag{2}$$

where S_0 and S_n are the initial and subsequent (final) cross-section areas of the swaged sample [mm^2], respectively, r is radius of the sample (in measured location) [mm], N is number of revolutions and t is thickness of the sample [mm].

4. CONCLUSIONS

The results of analyses of samples after two different deformation processing methods, swaging and HPT, showed that both the intensive plastic deformation methods resulted in a significant increase in microhardness. Microhardness increase was significant especially for the specimen deformed using HPT. However the values increased for both the deformed samples when compared to pre-compacted states. Microstructure observations support the measurements. The grain size got smaller than the size of the initial powder particles for both the deformed samples. However, grain refinement was significant especially for the HPT processed sample. Substantial residual porosity was observed for the swaged sample, with the distribution of pores present along particle boundaries. The HPT sample did not show any significant residual porosity. Calculations of the degree of deformation showed higher imposed strain for the sample processed by HPT compared to the sample processed by swaging.

AKNOWLEDGEMENT

This paper was created within the research project no. SP2015/89 of VŠB – Technical University of Ostrava, CZ.

REFERENCES

[1] KOCICH R., MACHÁČKOVÁ A., KUNČICKÁ L., FOJTÍK F. Fabrication and characterization of cold-swaged multilayered Al–Cu clad composites. Materials & Design, Vol. 71, 2015, pp. 36–47.

[2] ZHEREBTSOV S., KUDRYAVTSEV E., KOSTJUCHENKO S., MALYSHEVA S., SALISHCHEV G. Strength and ductility-related properties of ultrafine grained two-phase titanium alloy produced by warm multiaxial forging. Materials Science and Engineering A, Vol. 536, 2012, pp. 190–196.

[3] STOLYAROV V.V., ZHU Y.T., LOWE T.C., ISLAMGALIEV R.K., VALIEV R.Z. Processing nanocrystalline Ti and its nanocomposites from micrometer-sized Ti powder using high pressure torsion. Materials Science and Engineering A, Vol. 282, 2000, pp. 78–85.

[4] KOCICH R., KURSA M., MACHÁČKOVÁ A. FEA of Plastic Flow in AZ63 Alloy during ECAP Process. Acta Physica Polonica A, Vol. 122, 2012, pp. 581–587.

[5] SEMENOVA I.P., POLYAKOV A.V., RAAB G.I., LOWE T.C., VALIEV R.Z. Enhanced fatigue properties of ultrafine-grained Ti rods processed by ECAP-Conform. Journal of Materials Science, Vol. 47, 2012, pp. 7777–7781.

[6] KOCICH R., KUNČICKÁ L., MIHOLA M., SKOTNICOVÁ K. Numerical and experimental analysis of twist channel angular pressing (TCAP) as a SPD process. Materials Science and Engineering A, Vol. 563, 2013, pp. 86–94.

[7] KOCICH R., MACHÁČKOVÁ A., KUNČICKÁ L. Twist channel multi-angular pressing (TCMAP) as a new SPD process: Numerical and experimental study. Materials Science and Engineering A, Vol. 612, 2014, pp.445–55.

[8] MOHAMMED IQBAL U., SENTHIL KUMAR V.S. An analysis on effect of multipass twist extrusion process of AA6061 alloy. Materials and Design, Vol. 50, 2013, pp. 946–953.

[9] HUANG J., ZHU Y.T., ALEXANDER D.J., LIAO X., LOWE T.C., ASARO R.J. Development of repetitive corrugation and straightening. Materials Science and Engineering A, Vol. 371, 2004, pp. 35–9.

[10] YOU G.L., HO N.J., KAO P.W. Aluminum based in situ nanocomposite produced from Al-Mg-CuO powder mixture by using friction stir processing. Materials Letters, Vol. 100, 2013, pp. 219–222.

[11] KOCICH R., MACHÁČKOVÁ A., FOJTÍK F. Comparison of strain and stress conditions in conventional and ARB rolling processes. International Journal of Mechanical Sciences, Vol. 64, 2012, pp. 54–61.

[12] LOWE T.C., LIPKIN J. Analysis of axial deformation response during reverse shear. Journal of the Mechanics and Physics of Solids, Vol. 39, 1991, pp. 417–440.

[13] KHEREDDINE A.Y., LARBI F.H., KAWASAKI M., BAUDIN T., BRADAI D., LANGDON T.G. An examination of microstructural evolution in a Cu-Ni-Si alloy processed by HPT and ECAP. Materials Science and Engineering A, Vol. 576, 2013, pp. 149–155.

[14] NOURI A., HODGSON P.D., WEN C.E. Effect of process control agent on the porous structure and mechanical properties of a biomedical Ti-Sn-Nb alloy produced by powder metallurgy. Acta Biomaterialia, Vol. 6, 2010, pp. 1630–1639.

[15] AHMADZADEH H., FREEDMAN B.R., CONNIZZO B.K., SOSLOWSKY L.J., SHENOY V.B. Micromechanical poroelastic finite element and shear-lag models of tendon predict large strain dependent Poisson ' s ratios and fluid expulsion under tensile loading. Acta Biomaterialia, 2015, IN PRESS. Doi:10.1016/j.actbio.2015.04.035.

[16] GAN W.M., HUANG Y.D., WANG R., WANG G.F., SRINIVASAN A., BROKMEIER H.G., et al. Microstructures and mechanical properties of pure Mg processed by rotary swaging. Materials and Design, Vol. 63, 2014, pp. 83–88.

[17] PIPPAN R., SCHERIAU S., HOHENWARTER A., HAFOK M. Advantages and Limitations of HPT: A Review. Materials Science Forum, Vol. 584-586, 2008, pp. 16–21.

[18] JAHEDI M., KNEZEVIC M., PAYDAR M. H. High-Pressure double torsion as a severe plastic deformation process: Experimental Procedure and Finite Element Modeling. Journal of Materials Engineering and Performance, Vol. 24, 2015, pp. 1471-1482.

[19] CAO Y., WANG Y.B., FIGUEIREDO R.B., CHANG L., LIAO X.Z., KAWASAKI M., et al. Three-dimensional shear-strain patterns induced by high-pressure torsion and their impact on hardness evolution. Acta Materialia, Vol. 59, 2011, pp. 3903–3914.

[20] KOCICH R. SPD Metody, Od mikrometrů k nanometrům. 1st ed. Marionetti Press: Ostrava, 2011.

[21] BACHMAIER A., HAFOK M., SCHUSTER R., PIPPAN R. Limitations in the refinement by severe plastic deformation: The effect of Processing. Reviews on Advanced Materials Science, Vol. 25, 2010, pp. 16–22.